AMERICAN SOCIETY FOR MICROBIOLOGY | Applied and Environmental Microbiology

SPOTLIGHT

Articles of Significant Interest Selected from This Issue by the Editors

New Metagenome Assemblies Reveal Multiple Populations of Hydrothermal Vent Tubeworm Symbionts

Vestimentiferan tubeworms are hosts to intracellular, environmentally acquired, chemolithotrophic gammaproteobacterial symbionts. Phylogenetic analyses based on a few molecular markers seemed to indicate that nearly all of the Eastern Pacific host species were associated with the same symbiont phylotype, "*Candidatus* Endoriftia persephone." Using genome-wide comparisons of "*Candidatus* Endoriftia persephone" in association with three worm species, Perez and Juniper (p. 5197–5205) showed that Northeast Pacific and East Pacific Rise symbiont populations separated by mid-ocean ridge discontinuities were vicariant and that other factors (e.g., local environmental conditions, host specificity) may also shape the genetic makeup of these populations.

A New Source of Antimicrobials To Combat Antibiotic-Resistant Pathogens

Novel antimicrobials are critically needed to deal with the current global problems associated with antibiotic resistance in human and animal infections. Using a screening strategy for broad-spectrum antimicrobials combined with genome mining, Ovchinnikov et al. (p. 5216–5224) discovered a new group of antimicrobial peptides (bacteriocins) that show very potent activity against many important Gram-positive pathogens and their antibiotic-resistant derivatives. These bacteriocins differ from other known bacteriocins in terms of chemical composition and mechanism of action, thus representing great potential in diverse antimicrobial applications. The study also provides a useful strategy to search for novel antimicrobials.

Cell Surface Glycoside Hydrolases of *Streptococcus gordonii* Promote Growth in Saliva

Bacterial growth on salivary glycoproteins is critical for dental plaque biofilm development; however, little is known about how specific salivary components are utilized by different members of the oral bacterial community. The commensal bacterium *Streptococcus gordonii* DL1 has three cell wall-anchored glycoside hydrolases (GHs) predicted to degrade host glycans. Yang et al. (p. 5278–5286) constructed deletion mutants of the corresponding genes and compared mutants with the wild type for growth and glycan foraging in saliva. The results revealed that sequential action of these cell surface GHs on N-linked glycans of basic proline-rich salivary glycoproteins is an essential first step for growth of *S. gordonii* DL1 in saliva.

High-Pressure Germination of *Clostridium difficile* and *Clostridium perfringens* Spores

By triggering spore germination and then killing the less-resistant germinated spores, hydrostatic pressure (HP) treatment of foods can reduce levels of resistant spores of *Bacillus* or *Clostridium* species that cause food spoilage or foodborne disease. Most studies of HP germination have used spores of *Bacillus* species, while Doona and colleagues (p. 5287–5297) have studied the HP germination of spores of *Clostridium difficile* and *Clostridium perfringens*, which have significant impacts on human health. This work has provided new insight into how clostridial spores germinate under several HPs and has identified a pretreatment that can greatly increase HP germination of *C. perfringens* spores.

Inactivation of the 1,3-Propanediol Pathway in *Clostridium pasteurianum*

The synthesis of cell mass from glycerol by select *Clostridium* species is redox coupled with production of 1,3-propanediol. Inactivation of the 1,3-propanediol pathway in these organisms is expected to result in an inability to catabolize glycerol due to redox imbalance. Nevertheless, Pyne et al. (p. 5375–5388) demonstrated that biomass formation and glycerol utilization were unaffected by disruption of the 1,3-propanediol pathway in *Clostridium pasteurianum*, a specialized producer of *n*-butanol. The authors identified a novel 1,2-propanediol formation pathway that facilitates redox balance in the engineered mutant. This finding informs strain engineering and underscores the exceptional metabolic flexibility possessed by the clostridia.

doi:10.1128/AEM.02023-16

AMERICAN SOCIETY FOR MICROBIOLOGY | Applied and Environmental Microbiology

Disruption of the Reductive 1,3-Propanediol Pathway Triggers Production of 1,2-Propanediol for Sustained Glycerol Fermentation by *Clostridium pasteurianum*

Michael E. Pyne,[a]* Stanislav Sokolenko,[a] Xuejia Liu,[a] Kajan Srirangan,[a] Mark R. Bruder,[a] Marc G. Aucoin,[a] Murray Moo-Young,[a] Duane A. Chung,[a,b,c] C. Perry Chou[a]

Department of Chemical Engineering, University of Waterloo, Waterloo, Ontario, Canada[a]; Department of Pathology and Molecular Medicine, McMaster University, Hamilton, Ontario, Canada[b]; Neemo, Inc., Hamilton, Ontario, Canada[c]

ABSTRACT

Crude glycerol, the major by-product of biodiesel production, is an attractive bioprocessing feedstock owing to its abundance, low cost, and high degree of reduction. In line with the advent of the biodiesel industry, *Clostridium pasteurianum* has gained prominence as a result of its unique capacity to convert waste glycerol into *n*-butanol, a high-energy biofuel. However, no efforts have been directed at abolishing the production of 1,3-propanediol (1,3-PDO), the chief competing product of *C. pasteurianum* glycerol fermentation. Here, we report rational metabolic engineering of *C. pasteurianum* for enhanced *n*-butanol production through inactivation of the gene encoding 1,3-PDO dehydrogenase (*dhaT*). In spite of current models of anaerobic glycerol dissimilation, culture growth and glycerol utilization were unaffected in the *dhaT* disruption mutant (*dhaT*::Ll.LtrB). Metabolite characterization of the *dhaT*::Ll.LtrB mutant revealed an 83% decrease in 1,3-PDO production, encompassing the lowest *C. pasteurianum* 1,3-PDO titer reported to date (0.58 g liter^{-1}). With 1,3-PDO formation nearly abolished, glycerol was converted almost exclusively to *n*-butanol (8.6 g liter^{-1}), yielding a high *n*-butanol selectivity of 0.83 g *n*-butanol g^{-1} of solvents compared to 0.51 g *n*-butanol g^{-1} of solvents for the wild-type strain. Unexpectedly, high-performance liquid chromatography (HPLC) analysis of *dhaT*::Ll.LtrB mutant culture supernatants identified a metabolite peak consistent with 1,2-propanediol (1,2-PDO), which was confirmed by nuclear magnetic resonance (NMR). Based on these findings, we propose a new model for glycerol dissimilation by *C. pasteurianum*, whereby the production of 1,3-PDO by the wild-type strain and low levels of both 1,3-PDO and 1,2-PDO by the engineered mutant balance the reducing equivalents generated during cell mass synthesis from glycerol.

IMPORTANCE

Organisms from the genus *Clostridium* are perhaps the most notable native cellular factories, owing to their vast substrate utilization range and equally diverse variety of metabolites produced. The ability of *C. pasteurianum* to sustain redox balance and glycerol fermentation despite inactivation of the 1,3-PDO pathway is a testament to the exceptional metabolic flexibility exhibited by clostridia. Moreover, identification of a previously unknown 1,2-PDO-formation pathway, as detailed herein, provides a deeper understanding of fermentative glycerol utilization in clostridia and will inform future metabolic engineering endeavors involving *C. pasteurianum*. To our knowledge, the *C. pasteurianum dhaT* disruption mutant derived in this study is the only organism that produces both 1,2- and 1,3-PDOs. Most importantly, the engineered strain provides an excellent platform for highly selective production of *n*-butanol from waste glycerol.

As a result of a 6-fold increase in global production between 2005 and 2012, biodiesel is presently the second most common biofuel in the world next to ethanol (1). This dramatic increase has generated an exceptional surplus of crude glycerol (80% purity), which comprises 10% (wt/wt) of final biodiesel preparations. The price of crude glycerol plummeted to roughly €0 per ton in 2009, rendering it a waste stream rather than a once-valued coproduct of biodiesel production (2, 3). Although the waste feedstock has since found use in a range of industrial processes (4), leading to a modest rebound in price, impurities arising from the transesterification reaction, namely, methanol and free fatty acids, place constraints on the utilization of crude glycerol in many applications (5). The biotechnological avenue of glycerol valorization offers a myriad of opportunities, as many microorganisms are able to tolerate moderate levels of methanol and free fatty acids (6). Impurities can also be removed or inactivated using simple cost-effective means (7, 8). In addition to its low cost and abundance, glycerol is attractive from a fermentation perspective, owing to its high degree of reductance (γ_D, 4.67) compared to common sugar feedstocks, such as glucose or xylose (γ_D, 4). Accordingly, glycerol-fermenting organ-

Received 5 May 2016 **Accepted** 19 June 2016

Accepted manuscript posted online 24 June 2016

Citation Pyne ME, Sokolenko S, Liu X, Srirangan K, Bruder MR, Aucoin MG, Moo-Young M, Chung DA, Chou CP. 2016. Disruption of the reductive 1,3-propanediol pathway triggers production of 1,2-propanediol for sustained glycerol fermentation by *Clostridium pasteurianum*. Appl Environ Microbiol 82:5375–5388. doi:10.1128/AEM.01354-16.

Editor: M. J. Pettinari, University of Buenos Aires

Address correspondence to Duane A. Chung, duane.chung@uwaterloo.ca, or C. Perry Chou, cpchou@uwaterloo.ca.

* Present address: Michael E. Pyne, Department of Biology and Centre for Structural and Functional Genomics, Concordia University, Montréal, Québec, Canada.

isms produce a variety of highly reduced chemicals, including ethanol, 1,3-propanediol, and 2,3-butanediol.

Although many organisms in nature are capable of utilizing glycerol fermentatively as a sole source of carbon, *Clostridium pasteurianum* is the only organism that couples anaerobic glycerol catabolism with high-level production of *n*-butanol, a bulk chemical and prospective biofuel (9–11). *C. pasteurianum* is a strictly anaerobic endospore-forming apathogenic bacterium that can be cultivated in chemically defined medium and does not appear to be susceptible to strain degeneration processes that plague industrial exploitation of related clostridia (12). In contrast to common clostridial species, such as *Clostridium acetobutylicum* and *Clostridium beijerinckii*, *C. pasteurianum* has not been exploited industrially for large-scale production of solvents. Instead, biotechnological interest in *C. pasteurianum* has been spurred only recently in accordance with the tremendous growth experienced by the global biodiesel industry (11). Most organisms that metabolize glycerol fermentatively produce large amounts of 1,3-propanediol (1,3-PDO), the signature product of glycerol fermentation (13). Conversely, *C. pasteurianum* typically converts glycerol into equal amounts of 1,3-PDO and *n*-butanol (Fig. 1A). Given the organism's unique central metabolism, several studies have explored the glycerol-to-butanol fermentation carried out by *C. pasteurianum* (9–11). To enable metabolic engineering of *C. pasteurianum*, methodologies have recently been reported for electrotransformation (14), group-II-intron-mediated gene disruption (15), gene deletion and integration (16), antisense RNA (asRNA) gene knockdown (17), and clustered regularly interspaced short palindromic repeat (CRISPR)-associated (Cas) genome editing (18). We also sequenced the *C. pasteurianum* genome (19) and provided genomic analysis of the organism's central metabolism (20). *C. pasteurianum* genome sequences have been reported by at least five additional groups, covering the type strain (ATCC 6013/DSM 525) (16, 21–23) and two nontype strains (BC1 and NRRL B-598) (24). A method for electroporation of a unique acetone-producing aerotolerant strain was also described recently (25), demonstrating widespread interest in *C. pasteurianum* as a biocatalyst for crude glycerol valorization. Despite these advancements, only two targeted mutant strains possessing improved *n*-butanol-producing or glycerol-utilizing properties have been described. We previously downregulated the primary *C. pasteurianum* hydrogenase-encoding gene (*hydA*) using asRNA and observed superior growth characteristics, as well as enhanced titers of the reduced end products *n*-butanol and ethanol (17). Concurrently, Sandoval et al. (16) employed random mutagenesis and directed evolution to identify the Spo0A master transcriptional regulator as a key target for gene inactivation. Deletion of the corresponding *spo0A* gene yielded improved glycerol dissimilation and *n*-butanol yields, as well as decreased levels of 1,3-PDO. Prior to the development of the *C. pasteurianum* molecular genetic toolkit, however, strain engineering efforts have employed random mutagenesis and laborious screening procedures (12, 26).

Although *C. pasteurianum* growth medium can be manipulated to favor 1,3-PDO as the chief fermentation end product, yielding titers up to 5 g liter^{-1} (27), other glycerol-utilizing organisms, particularly *Clostridium butyricum* (28, 29), are superior producers of 1,3-PDO in terms of both yield and titer. In this regard, the 1,3-PDO pathway becomes a prominent target for metabolic engineering to enhance *n*-butanol yield and selectivity. However, current models of glycerol dissimilation in clostridia dictate that the reductive 1,3-PDO pathway is essential for fermentative glycerol utilization by facilitating redox balance (9, 30). Whereas the production of *n*-butanol (degree of reductance [γ_D], 6.0) and ethanol (γ_D, 6.0) from glycerol represents redox-balanced pathways, the conversion of glycerol to biomass generates an excess of reducing equivalents, as cell mass (γ_D, 4.3) is more oxidized than glycerol (γ_D, 4.67) (Fig. 1B). Hence, in order to sustain glycerol fermentation, the cell must employ a means of oxidizing the surplus of reductant generated from cell mass formation, a requirement typically fulfilled by the 1,3-PDO (γ_D, 5.33) pathway in glycerol-fermenting species. This reductive pathway results in the net oxidation of 1 mol of NADH per 1 mol of 1,3-PDO formed. The fundamental redox role of the 1,3-PDO pathway is further evidenced from work involving metabolic engineering of *C. acetobutylicum* (30, 31). Although the wild-type strain is unable to utilize glycerol as a sole source of carbon, the introduction of a heterologous 1,3-PDO formation pathway provided the capacity to ferment glycerol without the use of cosubstrates. Finally, supplying *C. pasteurianum* with exogenous electric current was found to enhance the production of 1,3-PDO (32), thus offering additional justification for the role of this pathway in maintaining redox balance by disposing of excess reductant. Based on these reports, it is presumed that inactivation of the reductive 1,3-PDO pathway in *C. pasteurianum* would lead to an inability to ferment glycerol due to redox imbalance. An exception to this rationale is provided by the fermentative glycerol metabolism unveiled in *Escherichia coli* (33, 34), an organism lacking a 1,3-PDO pathway. In this case, production of 1,2-propanediol (1,2-PDO) ($\gamma_D = 5.33$), rather than 1,3-PDO ($\gamma_D = 5.33$), balances the excess of reducing equivalents generated from the conversion of glycerol to cell mass. The 1,2-PDO pathway branches from the ubiquitous methylglyoxal bypass and, in a manner similar to 1,3-PDO synthesis, results in the net oxidation of 1 mol of NADH per mole of 1,2-PDO formed (Fig. 1A).

In this report, we investigate inactivation of the 1,3-PDO pathway on fermentative glycerol utilization and end product distribution in *C. pasteurianum*. Despite current models of anaerobic glycerol utilization in clostridia, cell growth and glycerol catabolism were unaffected by disruption of the 1,3-PDO dehydrogenase gene (*dhaT*) in *C. pasteurianum*. In addition to elevated levels of *n*-butanol, the engineered mutant was found to exhibit, to our knowledge, the lowest 1,3-PDO titer by *C. pasteurianum* reported to date. Furthermore, inactivation of the 1,3-PDO pathway triggered the production of 1,2-PDO, illuminating a new model of glycerol utilization in the clostridia characterized by reciprocal 1,2- and 1,3-PDO pathways for maintenance of redox balance during fermentative glycerol dissimilation.

MATERIALS AND METHODS

Bacterial cultivation and electrotransformation. The bacterial strains and plasmids employed in this study are listed in Table 1. *C. pasteurianum* ATCC 6013 was obtained from the American Type Culture Collection (ATCC) and was cultivated anaerobically at 37°C without agitation. For routine culture growth, *C. pasteurianum* was grown in 2× YTG medium (pH 6.3) (15) which contained (per liter): 16 g of tryptone, 10 g of yeast extract, 5 g of glucose, and 4 g of NaCl. Static flask cultivations were performed in 50 ml of standard semidefined medium (9, 35), which contained (per liter): 2 g of $(NH_4)_2SO_4$, 1 g of yeast extract, 22 g of KH_2PO_4, 6.6 g of K_2HPO_4, 0.2 g of $MgSO_4{\cdot}7H_2O$, 20 mg of $CaCl_2{\cdot}2H_2O$, 5 mg of $FeSO_4{\cdot}7H_2O$, 2 ml of trace element solution SL7, 1 mg of resazurin, and 0.5 g of cysteine-HCl. The medium pH was 6.0 to 6.1 prior to sterilization.

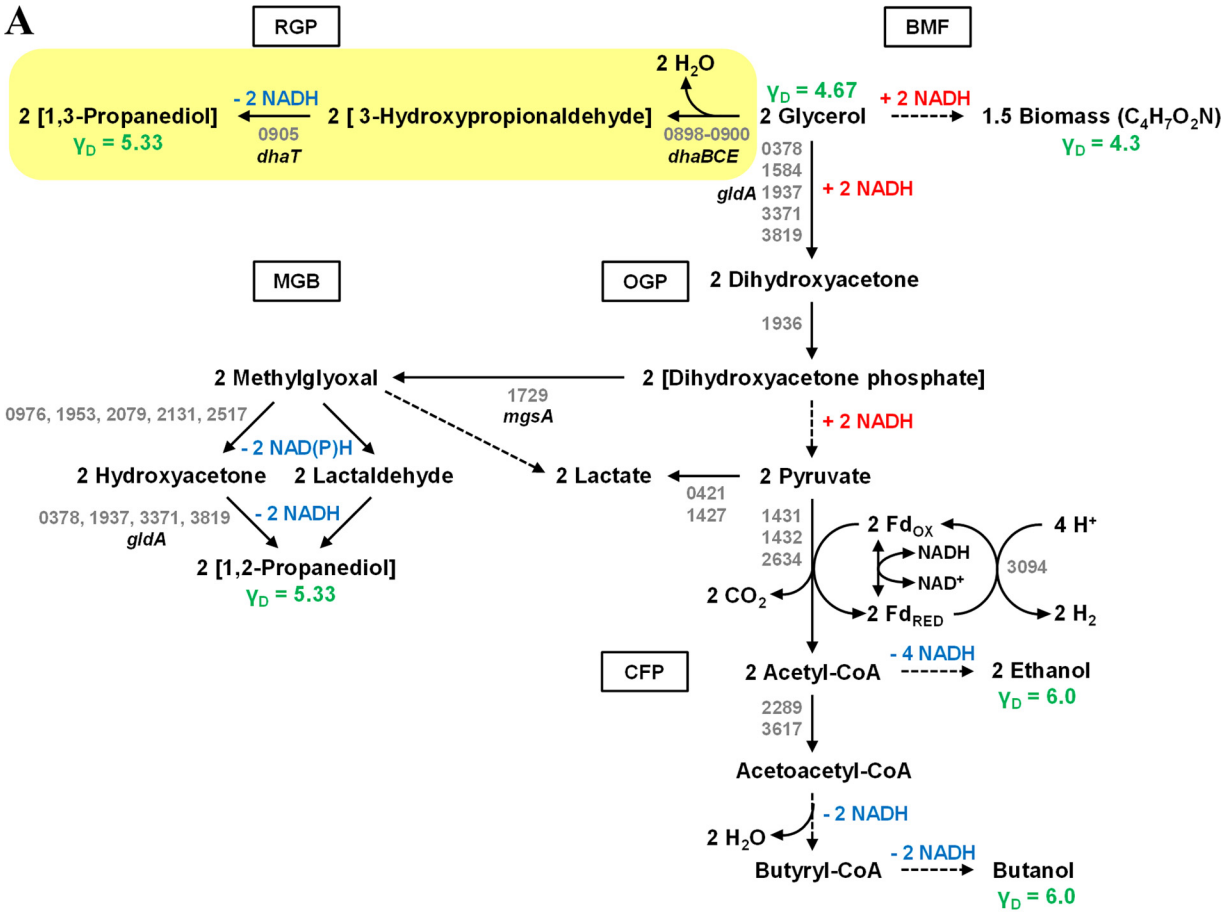

B

Glycerol catabolism balanced with ethanol formation

2 Glycerol → 2 Acetyl-CoA + 2 CO_2 + 2 H_2 + 4 NADH
2 Acetyl-CoA + 4 NADH → 2 Ethanol

2 Glycerol → 2 Ethanol + 2 CO_2 + 2 H_2

Glycerol catabolism balanced with butanol formation

2 Glycerol → 2 Acetyl-CoA + 2 CO_2 + 2 H_2 + 4 NADH
2 Acetyl-CoA + 4 NADH → Butanol + H_2O

2 Glycerol → Butanol + 2 CO_2 + 2 H_2 + H_2O

Biomass formation balanced with 1,3-propanediol production

4 Glycerol + NH_3 → 3 $C_4H_7O_2N$ + 6 H_2O + 4 NADH
4 Glycerol + 4 NADH → 4 [1,3-propanediol] + 4 H_2O

8 Glycerol + NH_3 → 3 $C_4H_7O_2N$ + 4 [1,3-propanediol] + 10 H_2O

Biomass formation balanced with 1,2-propanediol production

4 Glycerol + NH_3 → 3 $C_4H_7O_2N$ + 6 H_2O + 4 NADH
4 Glycerol → 4 DHAP + 4 NADH
4 DHAP + 8 NADH → 4 [1,2-propanediol]

8 Glycerol + NH_3 → 3 $C_4H_7O_2N$ + 4 [1,2-propanediol] + 6 H_2O

FIG 1 Fermentative glycerol utilization in *C. pasteurianum*. (A) Glycerol dissimilatory pathways probed and unveiled in this study. Pathways involved in production of ethanol, *n*-butanol, 1,2-PDO, and 1,3-PDO are shown. Acetate and butyrate formation pathways are omitted, and the reductive 1,3-PDO pathway targeted for inactivation is highlighted. Degree of reductance (γ_D) of glycerol and key end products is shown in green, while NADH-forming and NADH-consuming reactions are shown in red and blue, respectively. Locus tags (CP6013 prefix is omitted) corresponding to putative genes involved in key enzymatic steps are shown in gray and are based on the *C. pasteurianum* genome sequence reported by Pyne et al. (19, 20). Gene abbreviations are provided for select genes discussed in this study. For enzymatic reactions in which several paralogs exist, locus tags for up to five promising candidates are provided. Putative locus tags are provided for the presumed route of 1,2-PDO formation only (via hydroxyacetone). Dashed arrows represent multiple enzymatic conversions. BMF, biomass formation; CFP, central fermentative pathways; CoA, coenzyme A; *dhaBCE*, glycerol dehydratase gene; *dhaT*, 1,3-PDO dehydrogenase gene; FD_{OX}, oxidized ferredoxin; FD_{RED}, reduced ferredoxin; *gldA*, glycerol dehydrogenase gene; MGB, methylglyoxal bypass; *mgsA*, methylglyoxal synthase gene; OGP, oxidative glycerol pathway; RGP, reductive glycerol pathway. (B) Fermentation balances of glycerol utilization and end product formation in *C. pasteurianum*. Production of ethanol and *n*-butanol is shown balanced with glycerol consumption (left), whereas production of 1,2- and 1,3-propanediol is shown balanced with biomass formation (right). NADH formation and consumption are shown in red and blue, respectively.

Glycerol was autoclaved separately as a 200 g liter^{-1} stock solution and added to a final concentration of 40 g liter^{-1} in flasks containing 50 ml of medium. Prior to inoculation, biotin, *p*-aminobenzoic acid (PABA), and vitamin B_{12} were added to final concentrations of 0.02 mg liter^{-1}, 0.02 mg liter^{-1}, and 2 mg liter^{-1}, respectively. Concentrations of $(NH_4)_2SO_4$ (7.35 g liter^{-1}), $FeSO_4 \cdot 7H_2O$ (60 mg liter^{-1}), and yeast extract (5.08 g liter^{-1}) were increased in the medium formulation optimized for *n*-butanol production (27). Cultures of recombinant *C. pasteurianum* contained 5 μg

TABLE 1 Strains and plasmids employed in this study

Strains or plasmid	Relevant characteristics[a]	Source or reference
Strains		
Escherichia coli DH5α	F$^-$ *endA1 glnV44 thi-1 recA1 relA1 gyrA96 deoR nupG* Φ80d*lacZ*ΔM15 Δ(*lacZYA-argF*)*U169 hsdR17*(r_K^- m_K^+) λ^-	Lab stock
E. coli ER1821	F$^-$ *endA1 glnV44 thi-1 relA1?* e14$^-$(*mcrA*) *rfbD1? spoT1?* Δ(*mcrC-mrr*)*114*::IS*10*	Lab stock; New England Biolabs
Clostridium pasteurianum ATCC 6013	Wild type	American Type Culture Collection
Clostridium pasteurianum dhaT::Ll.LtrB	Disruption mutant generated by inserting the Ll.LtrB intron into position 503a of the *dhaT* gene encoding 1,3-propanediol dehydrogenase	This study
Plasmids		
pFnuDIIMKn	M.FnuDII methyltransferase plasmid for methylation of *E. coli-C. pasteurianum* shuttle vectors (Km^r; p15A ori)	14
pMTL85141ermB	*E. coli-Clostridium* shuttle vector (Cm^r/Tm^r Em^r; ColE1 ori; pIM13 ori)	14
pSY6catP-ltrA	Ll.LtrB deletion derivative of pSY6catP	15
pSYltrA	Control plasmid expressing the LtrA IEP and lacking the Ll.LtrB intron	15
pSYCP	*C. pasteurianum* intron disruption plasmid expressing the Ll.LtrB intron and LtrA IEP from the *C. pasteurianum* thiolase promoter.	15
pSYCP-dhaC(391a)	Intron disruption plasmid targeting site 391a within the *dhaC* coding sequence	This study
pSYCP-dhaT(503a)	Intron disruption plasmid targeting site 503a within the *dhaT* coding sequence	This study
pSYCP-dhaB(664s)	Intron disruption plasmid targeting site 664s within the *dhaB* coding sequence	This study
pSYCP-dhaB(758a)	Intron disruption plasmid targeting site 758a within the *dhaB* coding sequence	This study
pMTLdhaT	*dhaT* complementation plasmid expressing the *C. pasteurianum dhaT* gene from its native promoter	This study

[a] Km^r, kanamycin resistant; Cm^r, chloramphenicol resistant; Tm^r, thiamphenicol resistant; Em^r, erythromycin resistant; ?, unknown activity. The notation concerning *mcrA* indicates a loss of function.

ml^{-1} thiamphenicol or 2 μg ml^{-1} clarithromycin. *C. pasteurianum* was electrotransformed according to a previous report (14). Static flask fermentations were carried out for 96 to 120 h, at which time a single endpoint sample was removed for optical density at 600 nm (OD_{600}) measurement and metabolite analysis. *Escherichia coli* strains were grown aerobically at 37°C with agitation at 250 rpm in lysogeny broth (LB). *E. coli* strain DH5α was employed for plasmid construction and propagation, and strain ER1821 was utilized for *in vivo* methylation of *C. pasteurianum-E. coli* shuttle vectors using the gene encoding M.FnuDII methyltransferase expressed from the pFnuDIIMKn plasmid (14). Recombinant *E. coli* strains were selected using 100 μg ml^{-1} ampicillin, 30 μg ml^{-1} chloramphenicol, or 30 μg ml^{-1} kanamycin, whereby antibiotic concentrations were reduced by 50% for strains harboring two plasmids.

DNA isolation and manipulation. The oligonucleotides employed in this study were purchased from Integrated DNA Technologies (IDT; Coralville, IA) and are listed in Table 2. DNA manipulation was employed using established methods (36). Restriction endonucleases and Phusion and *Taq* DNA polymerases were purchased from New England BioLabs (NEB; Ipswich, MA). Commercial DNA purification and agarose gel extraction kits were obtained from Bio Basic, Inc. (Markham, Ontario, Canada). *C. pasteurianum* genomic DNA was isolated using a Qiagen DNeasy blood and tissue kit (Venlo, The Netherlands).

Plasmid pSYCP (15), expressing the Ll.LtrB group II intron and LtrA intron-encoded protein (IEP), was retargeted to 1,3-PDO pathway genes by reprogramming the Ll.LtrB intron using synthetic gBlock gene fragments or splicing by overlap extension-PCR (SOE-PCR). Synthetic gBlocks were purchased for intron retargeting to *dhaC*(391a) and *dhaT*(503a), amplified using primers pSYCP-gBlock.XhoI.S and pSYCP-gBlock.BsrGI.AS, and cloned into the XhoI and BsrGI sites of plasmid pSYCP, yielding pSYCP-dhaC(391a) and pSYCP-dhaT(503a), respectively. (Terms in parentheses represent predicted intron insertion sites, where "s" indicates sense and "a" indicates antisense.) Intron retargeting to *dhaB*(664s) in plasmid pSYCP-dhaB(664s) and *dhaB*(758a) in plasmid pSYCP-dhaB(758a) was achieved by SOE-PCR using primer sets dhaB(664s).IBS and EBS.Universal, and dhaB(664s).EBS2 and dhaB(664s).EBS1d for target site *dhaB*(664s), and primer sets dhaB (758a).IBS and EBS.Universal, and dhaB(758a).EBS2 and dhaB(758a). EBS1d for target site *dhaB*(758a). Full-length mutated PCR products were gel purified and cloned into the XhoI and BsrGI sites of plasmid pSYCP. A *dhaT* gene complementation plasmid, pMTLdhaT, was derived by PCR amplifying the native *dhaT* gene promoter and coding sequence from *C. pasteurianum* genomic DNA using primers dhaT.PvuI.S and dhaT. PvuI.AS. The resulting 1.5-kb PCR product was cloned into the PvuI site within plasmid pMTL85141ermB.

Intron-mediated gene disruption, enrichment, and plasmid curing. Disruption of 1,3-PDO pathway genes using targeted Ll.LtrB intron constructs was performed as previously described (15). Predicted intron insertion sites were identified and ranked using an algorithm from Targe Tronics, LLC (Austin, TX). Following intron reprogramming within pSYCP, approximately 5 to 10 μg of plasmid DNA was transferred to *C. pasteurianum* by electrotransformation. Transformants were initially screened for intron disruption using one locus-specific and one intron-specific primer to identify colonies harboring a chromosomal intron insertion. These colonies were further screened using locus-specific primers

TABLE 2 Oligonucleotides employed in this study

Oligonucleotide	Sequence (5′–3′)[a]
pSYCP-gBlock.XhoI.S	ATAACAATCGATTTGTGTATTTACTCGAGATAATTATCCTTA
pSYCP-gBlock.BsrGI.AS	CTCCTACAGATTGTACAAATGTGGTGATAACAG
dhaB(664s).IBS	ATTTACTCGAGATAATTATCCTTAGTTATCCTGAGAGTGCGCCCAGATAGGGTG
EBS.Universal	CGAAATTAGAAACTTGCGTTCAGTAAC
dhaB(664s).EBS2	TGAACGCAAGTTTCTAATTTCGATTATAACTCGATAGAGGAAAGTGTCT
dhaB(664s).EBS1d	CAGATTGTACAAATGTGGTGATAACAGATAAGTCCTGAGACTTAACTTACCTTTCTTTGT
dhaB(758a).IBS	ATTTACTCGAGATAATTATCCTTACTCATCTTTAATGTGCGCCCAGATAGGGTG
dhaB(758a).EBS2	TGAACGCAAGTTTCTAATTTCGATTATGAGTCGATAGAGGAAAGTGTCT
dhaB(758a).EBS1d	CAGATTGTACAAATGTGGTGATAACAGATAAGTCTTTAATCCTAACTTACCTTTCTTTGT
dhaT.PvuI.S	GGAGTACGATCGGGAACTGTAGAAGAAGATATGTCTATTGC
dhaT.PvuI.AS	ATTAAACGATCGCTTTATACAATAATACCCCTACAGCATCTCC
ARB1	GGCCACGCGTCGACTAGTACNNNNNNNNNNCTGC
ARB2	GGCCACGCGTCGACTAGTACNNNNNNNNNNGACTA
ARB3	GGCCACGCGTCGACTAGTACNNNNNNNNNNCATCA
ARB4	GGCCACGCGTCGACTAGTACNNNNNNNNNNCAAGA
ARB5	GGCCACGCGTCGACTAGTACNNNNNNNNNNATGAA
ltrB.Fw	CCAACGCGTCGCCACGTAATAAAT
ARB.nested	GGCCACGCGTCGACTAGTAC
ltrB.Fw2	CTCTATCGATCGCTAATCGAAATTAGAAACTTGCGTTCAG
dhaT.Fw	ATTGCAGCTACACACGAGGGAGAT
ltrB.Rv	ATGGGAACGAAACGAAAGCGATGC
dhaT.Rv	GGTTTGCATCTTTAGAAACATAGGACTC
dhaC.Fw	GGTTCTGGAATAGGTATTGGTATTC

[a] Underlined sequences represent relevant restriction endonuclease recognition sequences.

flanking the intron insertion site to determine if colonies were mosaic or harbored a homogeneous population of intron disruptants (15). Mosaic colonies were subjected to 10 rounds of intron enrichment in selective 2× YTG medium, and serial dilutions were plated on selective 2× YTG agar plates. Enrichment colonies were then PCR screened for intron insertion using locus-specific primers flanking the predicted intron insertion site. Intron insertion was deemed unsuccessful if colonies generated a wild-type PCR product or a mixture of wild-type and intron insertion products. Curing of plasmid pSYCP-dhaT(503a) was attempted through seven transfers in nonselective 2× YTG medium, as described previously (15). Colonies were then patched onto nonselective and selective 2× YTG agar plates to assess curing.

Identification of ectopic intron insertion by arbitrary colony PCR. Ectopic intron insertion within the *dhaT*::Ll.LtrB mutant strain was assessed using arbitrary colony PCR according to a previous method (37). A first round of PCR using *Taq* DNA polymerase was performed using one of five partially degenerate arbitrary PCR primers (ARB1 to ARB5; 5 μM final concentration) with primer LtrB.Fw (0.5 μM final concentration). Roughly 0.5 μl of these reaction mixtures was utilized as the template in a second PCR using *Taq* DNA polymerase and primers ARB.nested and LtrB.Fw2. Products were column purified and sequenced using primer LtrB.Fw2. DNA sequence flanking the Ll.LtrB intron region was queried against the *C. pasteurianum* genome using BLAST.

Analytical methods. Growth of static flask cultures was assessed by measuring the OD_{600} using a Beckman Coulter DU 520 spectrophotometer (Fullerton, CA). Concentrations of glycerol, acetate, lactate, butyrate, ethanol, *n*-butanol, and 1,3-propanediol were determined using a Shimadzu LC-10AT HPLC (Kyoto, Japan) equipped with an RID-10A refractive index detector and an Aminex HPX-87H column from Bio-Rad Laboratories (Richmond, CA). The mobile phase consisted of 5 mM H_2SO_4 (pH 2.0) maintained at a flow rate of 0.6 ml min^{-1}. Data processing was performed using Clarity Lite from DataApex (Prague, Czech Republic). The production of 1,2-PDO was validated and quantified using NMR, as previously described (38). Briefly, culture samples were prepared for analysis by adding an internal standard to bring the sample up to 10% (vol/vol) D_2O and 0.5 mM DSS (4,4-dimethyl-4-silapentane-1-sulfonic acid). The samples were scanned on a Bruker Avance 600 MHz spectrometer with triple resonance probe (TXI 600) using the first increment of a one-dimensional (1D)-nuclear Overhauser effect spectroscopy (NOESY) pulse sequence. Spectra were analyzed using Chenomx NMR Suite 8.0 (Edmonton, Alberta, Canada). Compound concentrations were calculated from the areas of ideal NMR peaks generated from the software library and superimposed on the observed spectra. 1,3-Propanediol was added to the library using the Compound Builder utility.

RESULTS

Intron-mediated disruption of the 1,3-PDO pathway genes. To probe the glycerol catabolic pathways of *C. pasteurianum* and enhance *n*-butanol selectivity through rational metabolic engineering, we set out to disrupt the reductive 1,3-propanediol (1,3-PDO) formation pathway in *C. pasteurianum*. We recently adapted the clostridial group II intron gene disruption system for use in *C. pasteurianum* (15), which employs plasmid pSYCP expressing the Ll.LtrB group II intron and LtrA intron-encoded protein. The conversion of glycerol to 1,3-PDO involves a two-step transformation by glycerol dehydratase (DhaBCE), encoded by *dhaBCE*, and 1,3-PDO dehydrogenase (DhaT), encoded by *dhaT* (Fig. 1A). We targeted both genes for inactivation through programming of the mobile Ll.LtrB intron within pSYCP to chromosomal target sites *dhaB*(664s), *dhaB*(758a), *dhaC*(391a), and *dhaT*(503a). Collectively, the predicted intron insertion sites possessed scores of 6.1 to 7.8 and targeted both sense (S) and antisense (AS) strands of the *C. pasteurianum* 1,3-PDO regulon. The corresponding plasmids pSYCP-dhaB(664s), pSYCP-dhaB(758a), pSYCP-dhaC(391a), and pSYCP-dhaT(503a) were used to transform *C. pasteurianum*. All four gene disruption plasmids produced poor transformation efficiencies and led to abnormal colony morphologies compared to a control intron vector targeting the *C. pasteurianum cpaAIR* restriction endonuclease gene (pSYCP-cpaAIR) (15). The transformants harboring pSYCP-dhaC(391a) exhibited the most irregular colony morphology,

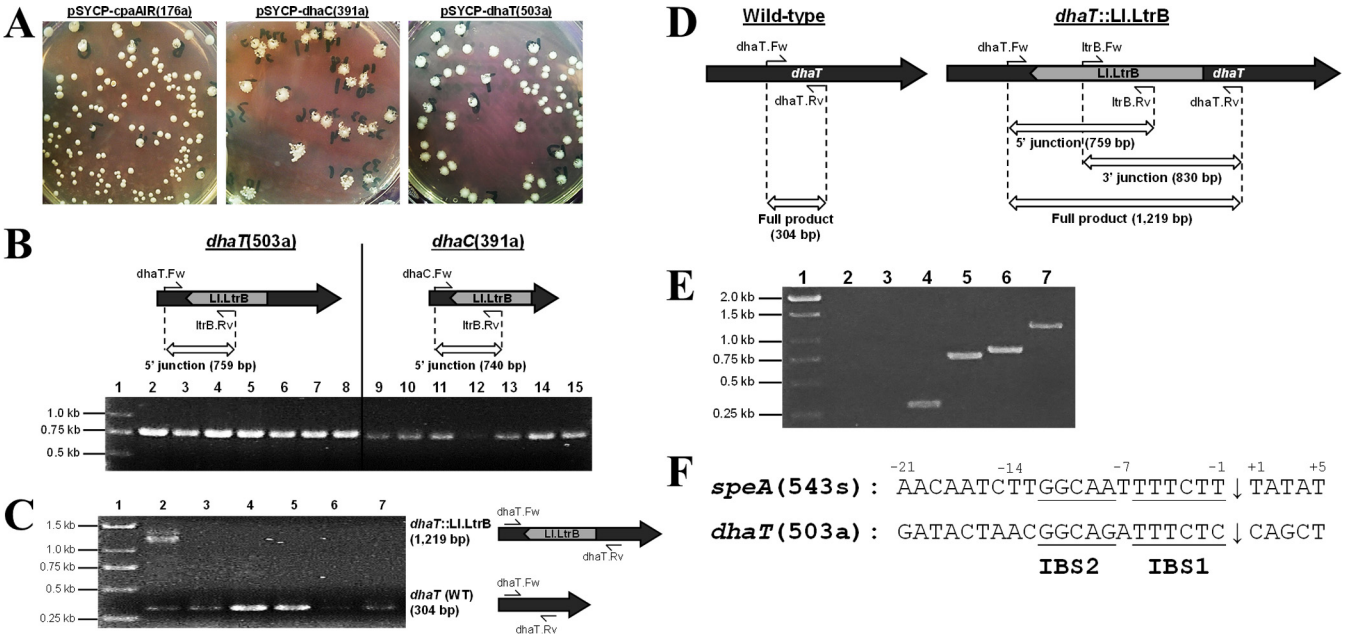

FIG 2 Confirmation of mosaic and homogeneous intron disruption in *C. pasteurianum dhaC* and *dhaT* genes, respectively. (A) Colony morphology of transformants harboring intron donor constructs targeting sites *cpaAIR*(176a), *dhaC*(391a), and *dhaT*(503a). (B) Genomic verification of *dhaT*(503a) and *dhaC*(391a) intron insertion using one locus-specific primer and one intron-specific primer. Lane 1, marker; lanes 2 to 8, pSYCP-dhaT(503a) transformants; lanes 9 to 15, pSYCP-dhaC(391a) transformants. (C) Confirmation of mosaic intron insertion at site *dhaT*(503a) using locus-specific primers flanking the predicted intron insertion site. Lane 1, marker; lanes 2 to 7, pSYCP-dhaT(503a) transformants. The transformant screened in lane 2 shows a mosaic intron insertion. (D) Expected PCR products of the wild-type (left) and *dhaT*::Ll.LtrB mutant (right) strain. Insertion of the Ll.LtrB intron into the *dhaT* gene leads to a 915-bp increase in size of the full-length PCR product generated using primers flanking the 503a intron insertion site (dhaT.Fw and dhaT.Rv). Both 5′- and 3′-gene-intron junction PCR products can be detected in *dhaT*::Ll.LtrB mutant cells using primer sets dhaT.Fw and ltrB.Rv, and ltrB.Fw and dhaT.Rv, respectively. (E) Genomic verification of a single positive *dhaT*::Ll.LtrB mutant colony by amplification of all three PCR products depicted in Fig. 2A (5′ junction, 3′ junction, and full product). A wild-type *C. pasteurianum* colony was included as a control for all three PCR primer sets. Lane 1, marker; lanes 2 to 4, wild-type colony; lanes 5 to 7, *dhaT*::Ll.LtrB mutant colony; lanes 2 and 5, 5′ junction; lanes 3 and 6, 3′ junction; lanes 4 and 7, full product. (F) Comparison of chromosomal intron insertion sites corresponding to *speA*(543s) and *dhaT*(503a). The predicted intron insertion site is shown with an arrow. Sequence similarities in intron binding site 1 (IBS1) and IBS2 involved in intron base pairing with target DNA are underlined.

characterized by a flat nebulous shape and rough edges (Fig. 2A). Transformants of pSYCP-dhaT(503a) displayed the least-altered morphology, yet colonies were still distinct from those harboring the control plasmid pSYCP-cpaAIR. Nevertheless, seven transformant colonies were screened for intron insertion using one intron-specific primer and one locus-specific primer for each of the four *dha* regulon intron disruption plasmids. Several transformants (43% to 100%) corresponding to all four Ll.LtrB intron target sites produced a PCR product consistent with successful intron insertion. Notably, transformants harboring pSYCP-dhaT(503a) and pSYCP-dhaC(391a) produced the expected intron insertion product in 7/7 transformant colonies (Fig. 2B). However, subsequent PCR screening using two locus-specific primers flanking the predicted intron insertion sites produced wild-type products for all colonies screened corresponding to intron insertion sites *dhaB*(664s), *dhaB*(758a), and *dhaC*(391a) (data not shown). Conversely, one transformant harboring pSYCP-dhaT(503a) produced both wild-type and intron insertion PCR products using primers flanking the predicted *dhaT*(503a) intron insertion site (Fig. 2C). We have previously observed mosaic intron disruption colonies, composed of both wild-type and intron insertion cells, using the Ll.LtrB intron in *C. pasteurianum*, which we have ascribed to poor retrohoming efficiency in this host (15). In an attempt to isolate pure intron insertion mutants, we performed an intron enrichment procedure starting with one mosaic colony of each of the four pSYCP-dha disruption transformants. Following 10 successive transfers in selective 2× YTG medium, cultures were serially diluted and plated onto nonselective medium. Roughly 28 enrichment colonies from each *dha*-targeting transformation were subsequently screened for intron insertion using locus-specific primers flanking the intron insertion site. While target sites *dhaB*(664s), *dhaB*(758a), and *dhaC*(391a) produced the wild-type product in 100% of the colonies screened (data not shown), 1/24 *dhaT*(503a) enrichment colonies produced the expected intron insertion PCR product with no evidence of the wild-type product. This mutant colony was further validated by screening both overlapping chromosome-intron junctions (Fig. 2D and E) and Sanger DNA sequencing of the resulting products (data not shown). The resulting *C. pasteurianum* mutant strain was designated *dhaT*::Ll.LtrB.

Curing of pSYCP-dhaT(503a) and identification of *speA* ectopic intron insertion. Following construction and validation of the *C. pasteurianum dhaT*::Ll.LtrB mutant, we attempted to cure the strain of the pSYCP-dhaT(503a) intron donor plasmid. Using a previously reported procedure (15), one colony of the *dhaT*::Ll.LtrB mutant was transferred in nonselective 2× YTG medium three times, serially diluted, and spread onto nonselective 2× YTG agar plates. A total of 24 single colonies were then picked and

streaked onto nonselective and selective 2× YTG agar to assess plasmid curing. Although this method led to a curing efficiency of 50% for plasmid pSYCP-cpaAIR(176a) (15), all 24/24 *dhaT*::Ll.LtrB mutant colonies produced growth on selective 2× YTG agar. In a second attempt at plasmid curing, we subcultured the *dhaT*::Ll.LtrB mutant using 10 successive transfers and screened 16 resultant colonies for plasmid loss. Once again, all 16 colonies screened grew on selective 2× YTG agar. We attempted a final plasmid curing experiment by cultivating the *dhaT*::Ll.LtrB mutant under dramatically altered growth conditions in the event that specific medium components were responsible for our inability to cure mutant cells of the pSYCP-dhaT(503a) plasmid. In place of 2× YTG, we cultivated the *dhaT*::Ll.LtrB mutant in a semidefined medium (9) containing 1 g liter^{-1} yeast extract and 40 g liter^{-1} sodium gluconate as a carbon source. The *dhaT*::Ll.LtrB mutant was transferred eight times in nonselective semidefined medium, and 100 colonies were assessed for plasmid curing. All 100 colonies screened in this manner grew on selective semidefined agar, again indicating an inability to cure plasmid pSYCP-dhaT(503a) from the *dhaT*::Ll.LtrB mutant.

The inability to cure intron donor plasmid from intron-disrupted cells suggests that the intron has inserted into the sense strand of an essential gene (39). Whereby antisense-oriented intron insertions produce unconditional disruptions, as transcription from the target gene promoter generates the complement sequence of the intron RNA, introns inserted into the sense orientation are transcribed into functional intron RNA (40, 41). If a source of the LtrA IEP is present, such sense-oriented introns can then be spliced from target mRNA, leading to the production of an intact and functional protein product despite insertional inactivation at the DNA level. Hence, essential genes can only be disrupted using a sense-oriented intron and if a source of the LtrA protein is supplied to mediate RNA splicing (39). Since the *dhaT*(503a) insertion carried by the *dhaT*::Ll.LtrB mutant constitutes an antisense intron insertion, we speculated that in addition to the intended *dhaT* insertion, the mutant also accumulated an off-target intron insertion within the sense strand of a gene that is essential to *C. pasteurianum*. To address this hypothesis, we used arbitrary PCR to identify potential ectopic intron insertions, since the technique is widely employed to rapidly genotype mutants generated via random transposon mutagenesis (42). We utilized five partially degenerate arbitrary PCR primers (Table 2), along with an intron-specific primer to amplify small regions of DNA sequence flanking any intron insertion that may be present within the genome of the *dhaT*::Ll.LtrB mutant. The resulting PCR products were sequenced, and intron-flanking sequences obtained were queried against the *C. pasteurianum* genome using BLAST. While only one of five arbitrary PCR primers amplified sequence flanking the validated *dhaT*(503a) intron insertion site, the remaining four arbitrary PCR primers generated the same off-target sequence corresponding to the arginine decarboxylase (*speA*) coding sequence. The Ll.LtrB intron was found to be inserted in the same position within the *speA* gene [*speA*(543s)] in all four PCR products. A comparison of the nucleotide sequences flanking the *speA* intron insertion site to the *dhaT*(503a) target site unveiled substantial sequence similarity in the intron binding site 2 (IBS2) and IBS1 regions required for base pairing between Ll.LtrB intron RNA and target DNA (Fig. 2F). Importantly, Ll.LtrB insertion occurred in the sense strand of the *speA* coding sequence, providing justification for our inability to cure the *dhaT*::Ll.LtrB mutant of plasmid pSYCP-dhaT(503a). We propose that the *C. pasteurianum speA* gene is essential for growth under the conditions employed in this study, whereby intron-mediated *speA* disruption is conditional on the production of the LtrA protein from plasmid pSYCP-dhaT(503a). The presence of plasmid pSYCP-dhaT(503a) and, therefore, LtrA protein, facilitates excision of the Ll.LtrB intron from *speA* at the mRNA level, generating intact functional SpeA protein (39). On the other hand, the disruption of *dhaT* in the *dhaT*::Ll.LtrB mutant is permanent and stable, as the Ll.LtrB intron is incapable of splicing from antisense-oriented DNA insertions (40, 41). Given the inability to cure cells of the intron donor plasmid, we proceeded with a characterization of solvent production using the *dhaT*::Ll.LtrB mutant.

Solvent production by *C. pasteurianum dhaT*::Ll.LtrB in standard and butanol-optimized media. To assess the effect of *dhaT* disruption on the growth and product distribution of *C. pasteurianum*, we first performed static flask cultivations of wild-type and *dhaT*::Ll.LtrB mutant strains using a standard semidefined growth medium containing 40 g liter^{-1} glycerol and 1 g liter^{-1} yeast extract. Under these conditions, growth on glycerol as a sole source of carbon was unaffected by *dhaT* disruption in the *dhaT*::Ll.LtrB mutant compared to the wild-type strain, as the two cultures reached a similar final cell density (OD_{600}, 3.0 to 3.1) and consumed roughly the same amount of glycerol (approximately 28 g liter^{-1}). Conversely, metabolite analysis of culture supernatants revealed dramatic differences in the central fermentative metabolism between the engineered mutant and the wild-type strain (Table 3). Whereas the wild-type strain converted glycerol to nearly equal quantities of 1,3-PDO and *n*-butanol (4.6 and 5.5 g liter^{-1}, respectively), the *dhaT*::Ll.LtrB mutant produced 83% less 1,3-PDO (0.79 g liter^{-1}) and 29% more *n*-butanol (7.1 g liter^{-1}). Accordingly, wild-type *C. pasteurianum* utilized 47.7% and 19.4% of glycerol for *n*-butanol and 1,3-PDO production, respectively, while the *dhaT*::Ll.LtrB mutant converted 62.8% of substrate to *n*-butanol and only 3.4% to 1,3-PDO. *n*-Butanol selectivity in the engineered mutant was 0.74 g *n*-butanol g^{-1} of total solvents (butanol, ethanol, 1,2-PDO, and 1,3-PDO), compared to 0.43 g *n*-butanol g^{-1} of total solvents in the wild-type strain (butanol, ethanol, and 1,3-PDO), corresponding to 72% improvement. Both strains generated small amounts of ethanol (1.4 to 2.7 g liter^{-1}) and only trace amounts of acetate, lactate, and butyrate (0.07 to 0.31 g liter^{-1} of total acids). The *dhaT*::Ll.LtrB mutant was capable of growth in a chemically defined medium containing biotin and *p*-aminobenzoic acid (PABA) (data not shown), indicating that growth was not dependent on the presence of yeast extract.

In an attempt to complement DhaT deficiency in the *dhaT*::Ll.LtrB mutant, we transformed the engineered strain with plasmid pMTLdhaT containing the *C. pasteurianum dhaT* gene expressed from its native promoter. Although the DhaT rescue strain produced twice as much 1,3-PDO as the *dhaT*::Ll.LtrB mutant, the complementation was weak, since the wild-type strain produced almost 3-fold-higher levels of 1,3-PDO than the complemented strain (Table 3). While *n*-butanol production was enhanced in the *dhaT*::Ll.LtrB mutant compared to the wild-type strain, the *n*-butanol titer following *dhaT* complementation was similar to that in the wild-type strain, wherein roughly half of the consumed glycerol was metabolized to *n*-butanol. Based on these data, plasmid-borne *dhaT* was only partially effective in complementing inactivated *dhaT* in the engineered mutant.

To further limit 1,3-PDO levels and enhance *n*-butanol pro-

TABLE 3 HPLC metabolite analysis of the wild-type and *dhaT*::Ll.LtrB mutant strains of *C. pasteurianum* in standard and butanol-optimized growth media

Strain by medium type	Cultivation time (h)	Growth (OD_{600})	Glycerol consumed (g liter^{-1})	Products formed (g liter^{-1} [%])[a]				Carbon recovery in products (%)[c]	Butanol selectivity (g g^{-1})[d]
				Butanol	1,3-PDO	Ethanol	Acids[b]		
Standard growth medium									
Wild type	112	3.1	28.5	5.5 ± 0.9 (47.7)	4.6 ± 0.2 (19.4)	2.7 ± 0.9 (18.7)	0.07 ± 0.06 (0.4)	86.4	0.43
dhaT::Ll.LtrB mutant	97	3.0	28.0	7.1 ± 2.0 (62.8)	0.79 ± 0.31 (3.4)	1.4 ± 0.9 (9.7)	0.31 ± 0.16 (1.8)	79.1	0.74
dhaT::Ll.LtrB [pMTL*dhaT*]	107	2.8	24.4	5.0 ± 0.7 (50.9)	1.6 ± 0.2 (7.7)	2.6 ± 0.4 (21.3)	0.25 ± 0.07 (1.5)	81.9	0.54
Optimized growth medium									
Wild type	102	4.1	31.8	6.7 ± 0.4 (52.1)	3.6 ± 0.5 (13.7)	2.9 ± 1.6 (18.2)	0.72 ± 0.21 (3.6)	87.7	0.51
dhaT::Ll.LtrB mutant	94	4.8	32.6	8.6 ± 0.1 (65.5)	0.58 ± 0.07 (2.1)	0.7 ± 0.1 (4.3)	0.35 ± 0.07 (1.9)	75.4	0.83

[a] Product titers are reported as average ± standard deviation of the results from three biological replicates. The percent moles of glycerol consumed in the production of each metabolite is provided in parentheses.
[b] Combined titer of acetate, butyrate, and lactate.
[c] Calculated as the percent moles of carbon in total liquid products (including 1,2-PDO and excluding biomass and gaseous products) per mole of carbon in glycerol consumed.
[d] Reported as grams of *n*-butanol produced per gram of total solvents (butanol, ethanol, 1,2-PDO, and 1,3-PDO).

duction, we investigated product distribution of the *dhaT*::Ll.LtrB mutant in a growth medium previously optimized for *n*-butanol production and low-level 1,3-PDO formation (27). Static flask fermentations were again performed using the wild-type and *dhaT*::Ll.LtrB mutant strains in the medium containing 40 g liter^{-1} glycerol. Compared to the standard growth medium, both the wild-type and engineered strain grew to a higher final cell density (OD_{600}, 4.1 and 4.8, respectively) and consumed more glycerol (31.8 and 32.6 g liter^{-1}, respectively) in the optimized medium (Table 3). The optimized medium proved effective in enhancing *n*-butanol production, as the titers were increased by 22% and 21% in the wild-type and *dhaT*::Ll.LtrB mutant strains, respectively, compared to the standard medium. Conversely, the use of the optimized medium led to a further 28% decrease in 1,3-PDO titer in the wild-type strain and a 34% decline in the engineered mutant. Under these conditions, the *dhaT*::Ll.LtrB mutant converted 65.5% of glycerol into *n*-butanol yet only 2.1% into 1,3-PDO, yielding final titers of 8.6 g liter^{-1} *n*-butanol and 0.58 g liter^{-1} 1,3-PDO. *n*-Butanol selectivity was 0.83 g *n*-butanol g^{-1} of solvents in the engineered mutant and 0.51 g *n*-butanol g^{-1} of solvents in the wild-type strain, corresponding to a 63% increase.

Elucidation of glycerol catabolic pathways in *dhaT*::Ll.LtrB mutant. During HPLC analysis of fermentation samples taken from cultures of the *C. pasteurianum dhaT*::Ll.LtrB mutant, we observed a peak (approximate retention time of 17.3 min) that partially overlapped the peak corresponding to 1,3-PDO (approximate retention time of 17.8 min) (Fig. 3A). This peak was observed in all *dhaT*::Ll.LtrB mutant samples yet was not detected in any wild-type culture supernatants, suggesting that production of the unknown metabolite is linked to disruption of *dhaT*. In line with this hypothesis, the area of the unknown peak was reduced in two out of three replicates of the *dhaT*::Ll.LtrB[*dhaT*] complementation strain and was not detected in the remaining replicate. In a first attempt to elucidate the identity of the unknown compound, we analyzed HPLC retention times of pure standards corresponding to key metabolites and pathway intermediates produced by *C. pasteurianum* (9, 10, 43), as well as compounds associated with glycerol dissimilation in other glycerol-fermenting microorganisms (2, 44, 45). Candidate metabolites included 3-hydroxypropionaldehyde, 3-hydroxypropionate, 1,2-PDO, propionate, *n*-propanol, acetoin, acetone, and acrolein. HPLC standards of prospective metabolites were prepared, and retention times (Table 4) were compared against chromatograms corresponding to the *dhaT*::Ll.LtrB mutant. Since 3-hydroxypropionaldehyde is not available commercially, a retention time of 15.6 min was assumed based on a report by Rütti et al. (46) that employed the same HPLC conditions utilized in this study. Similarly, an approximate retention time of 27.25 min for acrolein was assumed based on a report by Schaefer et al. (47), using conditions similar to those employed here. Although DhaT catalyzes the reduction of 3-hydroxypropionaldehyde to 1,3-PDO, we did not detect a buildup of this intermediate in the *dhaT*::Ll.LtrB mutant. We also did not identify metabolites derived from 3-hydroxypropionaldehyde, such as acrolein and 3-hydroxypropionate. Of the candidate compounds screened using HPLC, only 1,2-PDO (17.3 min) exhibited a retention time similar to that of the unknown peak (17.3 min) in *dhaT*::Ll.LtrB mutant culture supernatants (Fig. 3B), although a cluster of other key metabolites, namely, propionate (17.5 min), acetoin (17.8 min), and 1,3-PDO (17.8 min), were found to coelute within a very narrow retention range

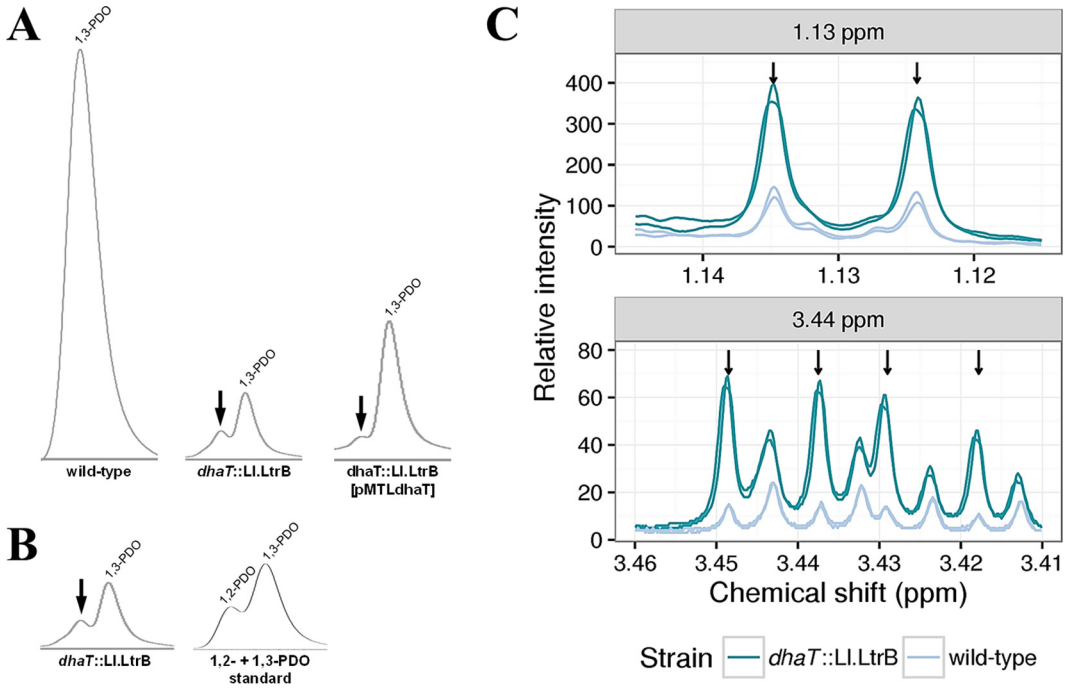

FIG 3 HPLC and NMR confirmation of 1,2-PDO production by *dhaT*::Ll.LtrB mutant. (A) Detection of a unique HPLC peak in supernatants derived from the *dhaT* disruption mutant (*dhaT*::Ll.LtrB) and the *dhaT*-complemented mutant (*dhaT*::Ll.LtrB[pMTLdhaT]). The HPLC peak corresponding to the unknown metabolite is shown with black arrows and was found to partially overlap the 1,3-PDO peak. The heights of the 1,3-PDO peaks are proportionate to the 1,3-PDO concentration. (B) Comparison of the unknown metabolite (arrow) and 1,3-PDO HPLC peaks in *dhaT*::Ll.LtrB mutant culture supernatants with pure standards of 1,2-PDO and 1,3-PDO at concentrations of 0.5 g liter^{-1} and 1.0 g liter^{-1}, respectively. The heights of the 1,3-PDO peaks are proportionate to 1,3-PDO concentration. (C) NMR resonances of 1,2-PDO used for identification and quantification. Arrows identify specific peaks attributed to 1,2-PDO. Spectra from two replicates of each strain are shown and were compared against a reference 1,2-PDO spectrum (not shown) from a standard chemical library. The chemical shift is depicted in parts per million (ppm) and is based on the change in standard resonance frequency of hydrogen (600 MHz).

of 17.5 to 17.8 min. To further resolve this cluster and identify the unknown metabolite produced by the *dhaT*::Ll.LtrB mutant, we subjected both wild-type and mutant culture samples to NMR analysis. NMR metabolite profiling revealed eight compounds that were present at substantially higher levels (approximately 100- to 1,000-fold) than all other metabolites in both wild-type and *dhaT*::Ll.LtrB mutant strain supernatants. As expected, these compounds included glycerol, formate, acetate, butyrate, ethanol, *n*-butanol, and 1,3-PDO. Among potential candidates, only 1,2-PDO was identified in all culture supernatants derived from the *dhaT*::Ll.LtrB mutant and, to a lesser extent, in culture samples of the wild-type strain (Fig. 3C). Despite some overlap with other chemical species, 1,2-PDO could be quantified using resonances at both 1.13 ppm and 3.44 ppm, with a 3.9-ppm resonance used for confirmation. Using the standard growth medium, 1,2-PDO production was found to be elevated 5-fold in the *dhaT*::Ll.LtrB mutant (0.30 ± 0.01 g liter^{-1}) relative to the wild-type organism (0.06 ± 0.00 g liter^{-1}). Cultivation of the engineered mutant in medium optimized for *n*-butanol production led to an increased 1,2-PDO titer of 0.43 ± 0.05 g liter^{-1}. Based on combined HPLC and NMR analyses, the identity of the unknown metabolite was unequivocally ascribed to 1,2-PDO. In other organisms, the 1,2-PDO pathway branches from the methylglyoxal bypass through two convergent pathways involving hydroxyacetone (acetol) or lactaldehyde (hydroxypropionaldehyde) (33, 48, 49) (Fig. 1A). Using pure standards to guide detection, we probed wild-type and *dhaT*::Ll.LtrB mutant culture supernatants for the presence of these intermediates using NMR. While the presence of lactaldehyde could not be confirmed or rejected, we observed resonances at 2.14 ppm and 4.37 ppm corresponding to the expected signals for hydroxyacetone based on spike-in experiments. In line with 1,2-PDO

TABLE 4 HPLC retention times of relevant metabolites and pathway intermediates discussed in this study

Metabolite	Approx retention time (min)	Reference
Lactate	12.6	This study
3-Hydroxypropionate	13.1	This study
Glycerol	13.9	This study
Acetate	15.0	This study
3-Hydroxypropionaldehyde[a]	15.6	46
Unknown *dhaT*::Ll.LtrB mutant peak	17.3	This study
1,2-Propanediol	17.4	This study
Propionate	17.5	This study
Acetoin	17.8	This study
1,3-Propanediol	17.8	This study
Butyrate	20.9	This study
Acetone	21.6	This study
Ethanol	22.2	This study
Acrolein[b]	27.2	47
Propanol	27.5	This study
Butanol	36.3	This study

[a] Retention time reported by Rütti et al. (46) under identical HPLC conditions.
[b] Retention time determined by Schaefer et al. (47) under similar HPLC conditions.

levels, hydroxyacetone concentration was elevated 4-fold in the engineered mutant (0.079 ± 0.05 mM) relative to the wild-type strain (0.019 ± 0.008 mM). Finally, we did not detect methylglyoxal in samples taken from either strain.

DISCUSSION

In this report, we describe the construction and characterization of a *C. pasteurianum* mutant strain possessing an inactivated 1,3-PDO formation pathway. Despite the requirement for 1,3-PDO production predicted by current metabolic models of glycerol fermentation in *Clostridium* and related microorganisms, inactivation of 1,3-PDO dehydrogenase (*dhaT*) did not affect growth of the organism on glycerol as a sole source of carbon and energy. Instead, we observed dramatically reduced levels of 1,3-PDO, which was compensated by elevated *n*-butanol production and activation of a previously unidentified 1,2-PDO formation pathway. This work embodies the lowest 1,3-PDO titer (0.58 g liter^{-1}) and one of the highest *n*-butanol selectivities (0.83 g *n*-butanol g^{-1} of solvents) reported to date for *C. pasteurianum*.

In response to inactivation of the 1,3-PDO pathway, the *dhaT*::Ll.LtrB mutant produced substantially more butanol (approximately 30%), likely a consequence of altered electron flow. As a *Clostridium* species, *C. pasteurianum* generates reductant in the form of NADH and reduced ferredoxin. During glycerol fermentation by the wild-type strain, NADH is predominantly used to drive the formation of butanol and 1,3-PDO. The fate of reduced ferredoxin is less implicit, as excess electrons can be "disposed of" through the formation of molecular hydrogen by the hydrogenase enzyme, or the reductant can be converted to NADH via ferredoxin:NAD$^+$ oxidoreductase. It has been shown that hydrogen evolution is dramatically reduced during clostridial glycerol fermentation due to induction of the ferredoxin:NAD$^+$ oxidoreductase enzyme, thus yielding additional NADH (50). With the 1,3-PDO and hydrogenase pathways largely inoperative, the *dhaT*::Ll.LtrB mutant was forced to overproduce butanol and activate the previously unidentified 1,2-PDO pathway to oxidize the excess NADH and sustain glycerol fermentation. In line with HPLC analysis, significant 1,2-PDO production (0.3 to 0.43 g liter^{-1}) by the *dhaT*::Ll.LtrB mutant strain was confirmed by NMR in this study (Fig. 3). While NMR also revealed trace amounts of 1,2-PDO in culture supernatants derived from the wild-type strain (0.06 g liter^{-1}), the levels were below the limit of detection using HPLC. Indeed, no prior studies have reported 1,2-PDO production by *C. pasteurianum*. Based on previous reports of fermentative glycerol utilization in *E. coli* (33, 34) and characterization of the *dhaT*::Ll.LtrB mutant in this study, we propose that the engineered mutant enlists both PDO pathways to consume reducing equivalents (i.e., NADH) generated in the synthesis of biomass during glycerol fermentation. Using a cell mass formula of $C_4H_7O_2N$ (9) and a dry cell weight of 0.26 g per OD_{600} for both *C. acetobutylicum* (51) and *C. beijerinckii* (52), the *dhaT*::Ll.LtrB mutant generated roughly 16.4 mM NADH through conversion of glycerol to biomass in the optimized growth medium. Thus, the formation of 16.4 mM 1,2-PDO and/or 1,3-PDO, equivalent to 1.2 g liter^{-1} total PDO, would be expected for the cell to restore redox balance (Fig. 1). Since the engineered strain produced 1.0 g liter^{-1} total PDO, it is apparent that the activity of both the 1,2- and 1,3-PDO pathways is necessary for sustaining glycerol catabolism in the engineered mutant. This outcome is corroborated by investigations into the anaerobic glycerol catabolism of *E. coli* (33), in which the production of only 0.04 g liter^{-1} 1,2-PDO was sufficient for balancing reducing equivalents generated from biomass formation. Although the *dhaT*::Ll.LtrB mutant derived in this study consumed approximately 4-fold more glycerol (32.6 g liter^{-1} compared to 8.1 g liter^{-1}) and grew to a 4-fold higher optical density (4.8 compared to 1.2, respectively) than *E. coli*, the *dhaT*::Ll.LtrB mutant produced roughly 28-fold more total PDO. Based on the above-described analyses, we propose that the activity of the dual PDO pathways provides sufficient means of balancing reducing equivalents generated in the synthesis of cell mass by the *dhaT*::Ll.LtrB mutant.

In the glycerol fermentation carried out by *E. coli* and other members of *Enterobacteriaceae*, 1,2-PDO production was found to be dependent on an oxidative type II glycerol dehydrogenase (glyDH-II) encoded by *gldA* (33). Whereas typical type I glycerol dehydrogenases oxidize glycerol to dihydroxyacetone, glyDH-II also plays an integral role in 1,2-PDO formation by reducing hydroxyacetone (acetol) to 1,2-PDO (Fig. 1A). The *C. pasteurianum* genome harbors five putative glycerol dehydrogenase genes (20), of which four of the corresponding proteins (loci CP6013_0378, CP6013_1937, CP6013_3371, and CP6013_3819) share 26% to 53% amino acid identities with glyDH-II from *E. coli* K-12 substrain MG1655 (locus b3945). At least one of these enzymes ostensibly mediates the production of 1,2-PDO in *C. pasteurianum*. The organism also harbors a single gene encoding methylglyoxal synthase (*mgsA*; locus CP6013_1729) for diversion of dihydroxyacetone phosphate from glycolysis to the methylglyoxal bypass (Fig. 1A). Methylglyoxal can then be converted to 1,2-PDO via hydroxyacetone (acetol) or lactaldehyde by sequential reduction reactions. In *Clostridium sphenoides*, 1,2-PDO is produced from lactaldehyde through the reduction of methylglyoxal by methylglyoxal reductase and 1,2-PDO dehydrogenase (49). In *E. coli* (33) and *Clostridium thermosaccharolyticum* (48), however, 1,2-PDO formation was found to proceed via hydroxyacetone through the action of an aldo-keto reductase, encoded by *yeaE*, *yghZ*, or *yafB* in *E. coli* (33), followed by glycerol dehydrogenase (*gldA*). Of these possible intermediates, we were successful in detecting only hydroxyacetone using NMR, suggesting that *C. pasteurianum* employs a pathway analogous to *E. coli* and *C. thermosaccharolyticum*. In this regard, *C. pasteurianum* harbors an assortment of genes encoding putative aldo-keto reductases (loci CP6013_0976, CP6013_1953, CP6013_2079, CP6013_2131, or CP6013_2517) for reduction of methylglyoxal to hydroxyacetone (Fig. 1A). The 1,2-PDO pathway in *E. coli* has been found to be induced under a very stringent set of bioprocessing conditions that includes low concentrations of potassium and phosphate, high concentrations of glycerol, acidic pH, and a low partial pressure of molecular hydrogen (33). In *C. sphenoides*, phosphate limitation alone is sufficient for triggering substantial production of 1,2-PDO (49), as the methylglyoxal bypass provides a nonglycolytic alternative devoid of phosphorylated intermediates. The *C. pasteurianum dhaT*::Ll.LtrB mutant in this study was cultivated in a medium containing very high concentrations of both potassium and phosphate (200 mM potassium phosphate buffer). While phosphate inhibits glycerol dehydrogenase (53) and methylglyoxal synthase (54, 55), both of which are key enzymes for 1,2-PDO formation, potassium enhances the toxicity of methylglyoxal (56), a highly toxic metabolite. Although glycerol utilization by the *dhaT*::Ll.LtrB mutant appeared to proceed unimpeded under these conditions (Table 3), it is possible that bioprocessing constraints were inadvertently

placed on the mutant's capacity for 1,2-PDO formation. Because the engineered strain continued to synthesize small amounts of 1,3-PDO despite the disruption of *dhaT*, it is probable that the 1,2-PDO pathway alone is insufficient for maintaining redox balance under the cultivation conditions employed. Instead, a small amount of 1,3-PDO production, presumably catalyzed by alternative iron-containing dehydrogenases exhibiting low-level activity on 3-hydroxypropionaldehyde, contributed to redox balance in the engineered mutant. Indeed, the *C. pasteurianum* genome encodes at least 13 iron-type alcohol dehydrogenases possessing significant similarity to the canonical DhaT amino acid sequence, providing justification for 1,3-PDO production despite *dhaT* inactivation. Given that multiple aldehyde-alcohol dehydrogenases are also involved in formation of butyraldehyde and *n*-butanol in *C. acetobutylicum* (57) and presumably *C. pasteurianum* (20), it may not be possible to completely abolish 1,3-PDO formation in the *dhaT*::Ll.LtrB mutant without compromising the strain's capacity for high level *n*-butanol formation. Hence, inactivation of the upstream gene encoding glycerol dehydratase (*dhaBCE*) and deletion of the entire 1,3-PDO regulon represent superior strategies for developing a completely 1,3-PDO-deficient mutant of *C. pasteurianum*. 1,3-PDO titers could be further decreased through inactivation of the Spo0A transcriptional regulator, as recently demonstrated by Sandoval et al. (16), resulting in enhanced glycerol utilization and decreased production of 1,3-PDO (Table 5). A number of promising *C. pasteurianum* strains have also been generated via random mutagenesis and directed evolution, such as the hyper *n*-butanol-producing strain described by Malaviya et al. (12). Implementation of *dhaT* inactivation in these strains might result in highly productive mutants for industrial production of *n*-butanol from waste glycerol.

Whereas *C. pasteurianum* is the only organism that combines fermentative glycerol utilization with high-level *n*-butanol production, *C. acetobutylicum* has been engineered for glycerol-to-butanol conversion through reconstitution of a full 1,3-PDO synthesis pathway from *Clostridium butyricum* (30, 31). Based on the model of clostridial glycerol utilization set forth in this study, wherein 1,2- and 1,3-PDO pathways exemplify complementary means of facilitating redox balance, it follows that *C. acetobutylicum* could be engineered for fermentative glycerol utilization through the introduction or activation of a functional 1,2-PDO formation pathway. Wild-type *C. acetobutylicum* harbors a methylglyoxal synthase gene (locus CA_C1604) (58), as well as multiple aldo-keto reductases (loci CA_C1958 and CA_C3378) sharing substantial amino acid identities with the corresponding proteins from *E. coli*. Although *C. acetobutylicum* also harbors a gene encoding glycerol dehydrogenase (locus CA_C1626), the corresponding protein bears little resemblance to the key glyDH-II glycerol dehydrogenase enzyme from *E. coli*. In principle, expression of the appropriate *C. pasteurianum* glycerol dehydrogenase gene in *C. acetobutylicum* could trigger 1,2-PDO synthesis, providing an alternative means of engineering *C. acetobutylicum* for fermentative glycerol utilization. In a broader sense, it would be of interest to determine how pervasive 1,2-PDO production is within the *Clostridium* genus and among glycerol utilizers in general. Evidence of 1,2-PDO formation by select clostridia has been reported, including *C. beijerinckii*, *C. difficile*, *C. sphenoides*, and *C. thermosaccharolyticum* (48, 49, 59), suggesting a ubiquitous role of the 1,2-PDO pathway in detoxifying methylglyoxal and surviving phosphate starvation, in addition to its function as a sink for re-

TABLE 5 Comparison of *C. pasteurianum* mutant strains constructed through rational metabolic engineering and random mutagenesis

Strain designation	Strain characteristic(s)	Products formed (g liter^{-1})			Butanol yield (g of *n*-butanol g^{-1} of glycerol consumed)	Butanol selectivity (g of *n*-butanol g^{-1} of total solvents)	Reference
		Butanol	1,3-PDO	Total solvents[a]			
ATCC 6013	Wild type	6.7	3.6	13.2	0.21	0.51	This study
dhaT::Ll.LtrB mutant	*dhaT* intron disruption mutant	8.6	0.58	10.3	0.26	0.83	This study
M150B[b]	Evolved strain (chemical mutagenesis)	7.1	1.5	9.1	0.18	0.78	16
Δ*spo0A* mutant[b]	*spo0A* deletion mutant	Comparable phenotype to evolved strain M150B	Comparable phenotype to evolved strain M150B	Comparable phenotype to evolved strain M150B	Comparable phenotype to evolved strain M150B	Comparable phenotype to evolved strain M150B	16
M150B	Evolved strain (chemical mutagenesis)	11.7	0.9	13.1	0.27	0.89	16
MBEL_GLY2	Evolved strain (chemical mutagenesis)	13.7	4.6	18.8	0.30	0.73	12
MBEL_GLY2[c]	Evolved strain (chemical mutagenesis)	17.3	9.5	27.4	0.30	0.63	12

[a] Includes *n*-butanol, ethanol, and 1,3-PDO. The strains assessed in this study (wild-type ATCC 6013 and *dhaT*::Ll.LtrB mutant) also include 1,2-PDO.
[b] Cultivated on crude glycerol.
[c] Cultivated under optimized conditions.

ducing equivalents as observed in wild-type *E. coli* and engineered *C. pasteurianum* strains.

Although both genes of the 1,3-PDO pathway (*dhaBCE* and *dhaT*) were targeted for disruption in this study, we were only successful in inactivating *dhaT*. Nevertheless, successful intron insertion was detected in all target sites assessed (Fig. 2B), including *dhaB* and *dhaC* subunits of the glycerol dehydratase gene, yet a pure *dhaBCE* inactivation mutant could not be isolated. Interestingly, mosaic *dhaB* and *dhaC* intron disruption colonies exhibited a highly irregular morphology, while colonies of the *dhaT*::Ll.LtrB mutant also appeared altered in appearance compared to a control intron insertional mutant (Fig. 2A). These data suggest that the 1,3-PDO pathway may be active or induced under standard growth conditions in the absence of glycerol, as the disruption of this pathway appears to affect colony morphology or overall cellular fitness. In glycerol-fermenting organisms, expression of the 1,3-PDO pathway is induced by dihydroxyacetone or glycerol (60), both of which are expected to be absent from the 2× YTG medium employed for gene disruption in this study. Given our difficulties in isolating a *dhaBCE* gene inactivation mutant using group II intron biology, this study also highlights the overall lack of robust genetic tools available for engineering *C. pasteurianum* and other solventogenic clostridia (15, 61). Indeed, the *dhaT* intron insertional mutant in this study was found to also harbor a conditional intron insertion in the *C. pasteurianum speA* gene, which we propose is essential for cell viability under the culture conditions employed. Because the Ll.LtrB intron is capable of splicing from the sense-oriented *speA* intron insertion but not from the antisense-oriented *dhaT* integration (39–41), it is highly unlikely that the off-target integration contributed to the phenotypic characteristics of the engineered *dhaT*::Ll.LtrB mutant. Additionally, plasmid-based complementation of *dhaT* proved to be only partially effective, again illuminating poor performance of clostridial genetic engineering tools. While plasmid stability has not been assessed in great detail in *C. pasteurianum*, the pIM13 plasmid replicon used for *dhaT* complementation in this study has been shown to be segregationally unstable in *Clostridium difficile* (62) and *Clostridium tyrobutyricum* (63). In the report on *C. tyrobutyricum*, the expression of an alcohol dehydrogenase from a pIM13-based plasmid led to slow culture growth, low enzyme activity, and overall poor alcohol titers compared to other plasmid replicons assayed (63). Such plasmid instability may have contributed to weak *dhaT* complementation in this study. To augment the growing clostridial molecular genetic toolbox, powerful and robust genome editing technologies based on CRISPR-Cas systems have recently been reported in a number of clostridia, including *C. beijerinckii* (64), *C. cellulolyticum* (65), and *C. pasteurianum* (18). A methodology based on homologous recombination and *mazF* counterselection has also been reported recently for use in engineering *C. pasteurianum* (16, 66). While the intron-based strategy employed in this study predates the advent of homologous-recombination-based techniques in *C. pasteurianum*, the availability of more-robust genome editing methods offers new opportunities for clostridial strain engineering. Indeed, the *C. pasteurianum dhaT* inactivation mutant constructed in this work exemplifies an exceptional chassis for further engineering toward the realization of an industrial bioprocess based on the conversion of low-value glycerol to *n*-butanol as a bulk chemical and prospective biofuel.

ACKNOWLEDGMENTS

We thank Jiri Perutka of TargeTronics for helpful discussions.

D.A.C. is a founder and employee of Neemo, Inc., at which M.E.P. has also been employed. Neemo, Inc. has a financial interest in the production of biofuels using *Clostridium*. The remaining authors declare no competing interests.

FUNDING INFORMATION

This work, including the efforts of C. Perry Chou, was funded by Canada Research Chairs (Chaires de Recherche du Canada) (CRC 950-211471). This work, including the efforts of C. Perry Chou, was funded by Gouvernement du Canada | Natural Sciences and Engineering Research Council of Canada (NSERC) (STPGP 430106). This work, including the efforts of C. Perry Chou, was funded by Gouvernement du Canada | Networks of Centres of Excellence of Canada (NCE).

The funding by Gouvernement du Canada | Networks of Centres of Excellence of Canada (NCE) was through the BioFuelNet research network.

REFERENCES

1. **US Energy Information Administration.** 2016. International energy statistics. US Energy Information Administration, Washington, DC. http://www.eia.gov/cfapps/ipdbproject/iedindex3.cfm.
2. **da Silva GP, Mack M, Contiero J.** 2009. Glycerol: a promising and abundant carbon source for industrial microbiology. Biotechnol Adv **27:** 30–39. http://dx.doi.org/10.1016/j.biotechadv.2008.07.006.
3. **Yazdani SS, Gonzalez R.** 2007. Anaerobic fermentation of glycerol: a path to economic viability for the biofuels industry. Curr Opin Biotechnol **18:**213–219. http://dx.doi.org/10.1016/j.copbio.2007.05.002.
4. **Yang FX, Hanna MA, Sun RC.** 2012. Value-added uses for crude glycerol–a byproduct of biodiesel production. Biotechnol Biofuels **5:**13. http://dx.doi.org/10.1186/1754-6834-5-13.
5. **Thompson JC, He BB.** 2006. Characterization of crude glycerol from biodiesel production from multiple feedstocks. Appl Eng Agric **22:**261–265. http://dx.doi.org/10.13031/2013.20272.
6. **Chatzifragkou A, Papanikolaou S.** 2012. Effect of impurities in biodiesel-derived waste glycerol on the performance and feasibility of biotechnological processes. Appl Microbiol Biotechnol **95:**13–27. http://dx.doi.org/10.1007/s00253-012-4111-3.
7. **Jensen TO, Kvist T, Mikkelsen MJ, Christensen PV, Westermann P.** 2012. Fermentation of crude glycerol from biodiesel production by *Clostridium pasteurianum*. J Ind Microbiol Biotechnol **39:**709–717. http://dx.doi.org/10.1007/s10295-011-1077-6.
8. **Wijesekara R, Nomura N, Sato S, Matsumura M.** 2008. Pre-treatment and utilization of raw glycerol from sunflower oil biodiesel for growth and 1,3-propanediol production by *Clostridium butyricum*. J Chem Technol Biotechnol **83:**1072–1080.
9. **Biebl H.** 2001. Fermentation of glycerol by *Clostridium pasteurianum*–batch and continuous culture studies. J Ind Microbiol Biotechnol **27:**18–26. http://dx.doi.org/10.1038/sj.jim.7000155.
10. **Dabrock B, Bahl H, Gottschalk G.** 1992. Parameters affecting solvent production by *Clostridium pasteurianum*. Appl Environ Microbiol **58:** 1233–1239.
11. **Taconi KA, Venkataramanan KP, Johnson DT.** 2009. Growth and solvent production by *Clostridium pasteurianum* ATCC (R) 6013 (TM) utilizing biodiesel-derived crude glycerol as the sole carbon source. Environ Prog Sustain Energy **28:**100–110. http://dx.doi.org/10.1002/ep.10350.
12. **Malaviya A, Jang YS, Lee SY.** 2012. Continuous butanol production with reduced byproducts formation from glycerol by a hyper producing mutant of *Clostridium pasteurianum*. Appl Microbiol Biotechnol **93:**1485–1494. http://dx.doi.org/10.1007/s00253-011-3629-0.
13. **Biebl H, Menzel K, Zeng A-P, Deckwer W-D.** 1999. Microbial production of 1, 3-propanediol. Appl Microbiol Biotechnol **52:**289–297. http://dx.doi.org/10.1007/s002530051523.
14. **Pyne ME, Moo-Young M, Chung DA, Chou CP.** 2013. Development of an electrotransformation protocol for genetic manipulation of *Clostridium pasteurianum*. Biotechnol Biofuels **6:**50. http://dx.doi.org/10.1186/1754-6834-6-50.
15. **Pyne ME, Moo-Young M, Chung DA, Chou CP.** 2014. Expansion of the genetic toolkit for metabolic engineering of *Clostridium pasteurianum*: chromosomal gene disruption of the endogenous CpaAI restriction en-

zyme. Biotechnol Biofuels **7:**163. http://dx.doi.org/10.1186/s13068-014-0163-1.
16. **Sandoval NR, Venkataramanan KP, Groth TS, Papoutsakis ET.** 2015. Whole-genome sequence of an evolved *Clostridium pasteurianum* strain reveals Spo0A deficiency responsible for increased butanol production and superior growth. Biotechnol Biofuels **8:**1. http://dx.doi.org/10.1186/s13068-014-0179-6.
17. **Pyne ME, Moo-Young M, Chung DA, Chou CP.** 2015. Antisense-RNA-mediated gene downregulation in *Clostridium pasteurianum*. Fermentation **1:**113–126. http://dx.doi.org/10.3390/fermentation1010113.
18. **Pyne ME, Bruder MR, Moo-Young M, Chung DA, Chou CP.** 2016. Harnessing heterologous and endogenous CRISPR-Cas machineries for efficient markerless genome editing in *Clostridium*. Sci Rep **6:**25666. http://dx.doi.org/10.1038/srep25666.
19. **Pyne ME, Utturkar S, Brown SD, Moo-Young M, Chung DA, Chou CP.** 2014. Improved draft genome sequence of *Clostridium pasteurianum* strain ATCC 6013 (DSM 525) using a hybrid next-generation sequencing approach. Genome Announc **2**(4):e00790-14. http://dx.doi.org/10.1128/genomeA.00790-14.
20. **Pyne ME, Liu X, Moo-Young M, Chung DA, Chou CP.** 2016. Genome-directed analysis of prophage excision, host defence systems, and central fermentative metabolism in *Clostridium pasteurianum*. Sci Rep **6:**26228.
21. **Poehlein A, Grosse-Honebrink A, Zhang Y, Minton NP, Daniel R.** 2015. Complete genome sequence of the nitrogen-fixing and solvent-producing *Clostridium pasteurianum* DSM 525. Genome Announc **3**(1):e01591-14. http://dx.doi.org/10.1128/genomeA.01591-14.
22. **Rappert S, Song L, Sabra W, Wang W, Zeng A-P.** 2013. Draft genome sequence of type strain *Clostridium pasteurianum* DSM 525 (ATCC 6013), a promising producer of chemicals and fuels. Genome Announc **1**(1): e00232-12. http://dx.doi.org/10.1128/genomeA.00232-12.
23. **Rotta C, Poehlein A, Schwarz K, McClure P, Daniel R, Minton NP.** 2015. Closed genome sequence of *Clostridium pasteurianum* ATCC 6013. Genome Announc **3**(1):e01596-14. http://dx.doi.org/10.1128/genomeA.01596-14.
24. **Kolek J, Sedláø K, Provazník I, Patáková P.** 2014. Draft genome sequence of *Clostridium pasteurianum* NRRL B-598, a potential butanol or hydrogen producer. Genome Announc **2**(2):e00192-14. http://dx.doi.org/10.1128/genomeA.00192-14.
25. **Kolek J, Sedlar K, Provaznik I, Patakova P.** 2016. Dam and Dcm methylations prevent gene transfer into *Clostridium pasteurianum* NRRL B-598: development of methods for electrotransformation, conjugation, and sonoporation. Biotechnol Biofuels **9:**1. http://dx.doi.org/10.1186/s13068-015-0423-8.
26. **Jensen TO, Kvist T, Mikkelsen MJ, Westermann P.** 2012. Production of 1,3-PDO and butanol by a mutant strain of *Clostridium pasteurianum* with increased tolerance towards crude glycerol. AMB Express **2:**44. http://dx.doi.org/10.1186/2191-0855-2-44.
27. **Moon C, Lee CH, Sang BI, Um Y.** 2011. Optimization of medium compositions favoring butanol and 1,3-propanediol production from glycerol by *Clostridium pasteurianum*. Bioresour Technol **102:**10561–10568. http://dx.doi.org/10.1016/j.biortech.2011.08.094.
28. **Biebl H, Marten S, Hippe H, Deckwer W-D.** 1992. Glycerol conversion to 1,3-propanediol by newly isolated clostridia. Appl Microbiol Biotechnol **36:**592–597.
29. **González-Pajuelo M, Andrade J, Vasconcelos I.** 2005. Production of 1,3-propanediol by *Clostridium butyricum* VPI 3266 in continuous cultures with high yield and productivity. J Ind Microbiol Biotechnol **32:**391–396. http://dx.doi.org/10.1007/s10295-005-0012-0.
30. **González-Pajuelo M, Meynial-Salles I, Mendes F, Soucaille P, Vasconcelos I.** 2006. Microbial conversion of glycerol to 1,3-propanediol: physiological comparison of a natural producer, *Clostridium butyricum* VPI 3266, and an engineered strain, *Clostridium acetobutylicum* DG1(pSPD5). Appl Environ Microbiol **72:**96–101. http://dx.doi.org/10.1128/AEM.72.1.96-101.2006.
31. **González-Pajuelo M, Meynial-Salles I, Mendes F, Andrade JC, Vasconcelos I, Soucaille P.** 2005. Metabolic engineering of *Clostridium acetobutylicum* for the industrial production of 1,3-propanediol from glycerol. Metab Eng **7:**329–336. http://dx.doi.org/10.1016/j.ymben.2005.06.001.
32. **Choi O, Kim T, Woo HM, Um Y.** 2014. Electricity-driven metabolic shift through direct electron uptake by electroactive heterotroph *Clostridium pasteurianum*. Sci Rep **4:**6961. http://dx.doi.org/10.1038/srep06961.
33. **Gonzalez R, Murarka A, Dharmadi Y, Yazdani SS.** 2008. A new model for the anaerobic fermentation of glycerol in enteric bacteria: trunk and auxiliary pathways in *Escherichia coli*. Metab Eng **10:**234–245. http://dx.doi.org/10.1016/j.ymben.2008.05.001.
34. **Murarka A, Dharmadi Y, Yazdani SS, Gonzalez R.** 2008. Fermentative utilization of glycerol by *Escherichia coli* and its implications for the production of fuels and chemicals. Appl Environ Microbiol **74:**1124–1135. http://dx.doi.org/10.1128/AEM.02192-07.
35. **Mallette MF, Reece P, Dawes EA.** 1974. Culture of *Clostridium pasteurianum* in defined medium and growth as a function of sulfate concentration. Appl Microbiol **28:**999–1003.
36. **Sambrook J, Fritsch EF, Maniatis T.** 1989. Molecular cloning, vol 2. Cold Spring Harbor Laboratory Press, Cold Spring Harbor, NY.
37. **O'Toole GA, Kolter R.** 1998. Initiation of biofilm formation in *Pseudomonas fluorescens* WCS365 proceeds via multiple, convergent signalling pathways: a genetic analysis. Mol Microbiol **28:**449–461. http://dx.doi.org/10.1046/j.1365-2958.1998.00797.x.
38. **Sokolenko S, Aucoin MG.** 2015. A correction method for systematic error in ^{1}H-NMR time-course data validated through stochastic cell culture simulation. BMC Syst Biol **9:**1. http://dx.doi.org/10.1186/s12918-014-0137-8.
39. **Yao J, Zhong J, Fang Y, Geisinger E, Novick RP, Lambowitz AM.** 2006. Use of targetrons to disrupt essential and nonessential genes in *Staphylococcus aureus* reveals temperature sensitivity of Ll.LtrB group II intron splicing. RNA **12:**1271–1281.
40. **Frazier CL, San Filippo J, Lambowitz AM, Mills DA.** 2003. Genetic manipulation of *Lactococcus lactis* by using targeted group II introns: generation of stable insertions without selection. Appl Environ Microbiol **69:**1121–1128. http://dx.doi.org/10.1128/AEM.69.2.1121-1128.2003.
41. **Karberg M, Guo HT, Zhong J, Coon R, Perutka J, Lambowitz AM.** 2001. Group II introns as controllable gene targeting vectors for genetic manipulation of bacteria. Nat Biotechnol **19:**1162–1167. http://dx.doi.org/10.1038/nbt1201-1162.
42. **Knobloch JK, Nedelmann M, Kiel K, Bartscht K, Horstkotte MA, Dobinsky S, Rohde H, Mack D.** 2003. Establishment of an arbitrary PCR for rapid identification of Tn*917* insertion sites in *Staphylococcus epidermidis*: characterization of biofilm-negative and nonmucoid mutants. Appl Environ Microbiol **69:**5812–5818. http://dx.doi.org/10.1128/AEM.69.10.5812-5818.2003.
43. **Rainey FA, Hollen BJ, Small A.** 2009. Genus I. *Clostridium*, p 738–830. *In* De Vos P, Garrity GM, Jones D, Krieg NR, Ludwig W, Rainey FA, Schleifer KH, Whitman WB (ed), Bergey's manual of systematic bacteriology, 2nd ed, vol 3. Springer, New York, NY.
44. **Forsberg CW.** 1987. Production of 1,3-propanediol from glycerol by *Clostridium acetobutylicum* and other *Clostridium* species. Appl Environ Microbiol **53:**639–643.
45. **Johnson DT, Taconi KA.** 2007. The glycerin glut: options for the value-added conversion of crude glycerol resulting from biodiesel production. Environ Prog Sustain Energy **26:**338–348. http://dx.doi.org/10.1002/ep.10225.
46. **Rütti D, Lacroix C, Jeremic T, Mathis M, Die A, Vollenweider S.** 2011. Development of a reversible binding process for *in situ* removal of 3-hydroxypropionaldehyde during biotechnological conversion of glycerol. Biochem Eng J **55:**176–184. http://dx.doi.org/10.1016/j.bej.2011.04.005.
47. **Schaefer L, Auchtung TA, Hermans KE, Whitehead D, Borhan B, Britton RA.** 2010. The antimicrobial compound reuterin (3-hydroxypropionaldehyde) induces oxidative stress via interaction with thiol groups. Microbiology **156:**1589–1599. http://dx.doi.org/10.1099/mic.0.035642-0.
48. **Cameron DC, Cooney CL.** 1986. A novel fermentation: the production of R(—)-1,2–propanediol and acetol by *Clostridium thermosaccharolyticum*. Nat Biotechnol **4:**651–654. http://dx.doi.org/10.1038/nbt0786-651.
49. **Tran-Din K, Gottschalk G.** 1985. Formation of D(—)-1, 2-propanediol and D(—)-lactate from glucose by *Clostridium sphenoides* under phosphate limitation. Arch Microbiol **142:**87–92. http://dx.doi.org/10.1007/BF00409243.
50. **Vasconcelos I, Girbal L, Soucaille P.** 1994. Regulation of carbon and electron flow in *Clostridium acetobutylicum* grown in chemostat culture at neutral pH on mixtures of glucose and glycerol J Bacteriol **176:**1443–1450.
51. **Liu L, Zhang L, Tang W, Gu Y, Hua Q, Yang S, Jiang W, Yang C.** 2012. Phosphoketolase pathway for xylose catabolism in *Clostridium acetobutylicum* revealed by ^{13}C metabolic flux analysis. J Bacteriol **194:**5413–5422. http://dx.doi.org/10.1128/JB.00713-12.
52. **Guo T, Tang Y, Zhang QY, Du TF, Liang DF, Jiang M, Ouyang PK.** 2012. *Clostridium beijerinckii* mutant with high inhibitor tolerance ob-

tained by low-energy ion implantation. J Ind Microbiol Biotechnol **39:** 401–407. http://dx.doi.org/10.1007/s10295-011-1017-5.
53. **Truniger V, Boos W.** 1994. Mapping and cloning of *gldA*, the structural gene of the *Escherichia coli* glycerol dehydrogenase. J Bacteriol **176:**1796–1800.
54. **Cooper R.** 1984. Metabolism of methylglyoxal in microorganisms. Annu Rev Microbiol **38:**49–68. http://dx.doi.org/10.1146/annurev.mi.38.100184.000405.
55. **Hopper D, Cooper R.** 1971. The regulation of *Escherichia coli* methylglyoxal synthase; a new control site in glycolysis? FEBS Lett **13:**213–216. http://dx.doi.org/10.1016/0014-5793(71)80538-0.
56. **Booth IR.** 2005. Glycerol and methylglyoxal metabolism. *In* Brock A, Curtiss R, III, Kaper JB, Neidhardt FC, Nystrom T, Rudd KE, Squires CL (ed), EcoSal-*Escherichia coli* and *Salmonella*: cellular and molecular biology. ASM Press, Washington, DC.
57. **Dürre P.** 2007. Biobutanol: an attractive biofuel. Biotechnol J **2:**1525–1534. http://dx.doi.org/10.1002/biot.200700168.
58. **Huang K-X, Rudolph FB, Bennett GN.** 1999. Characterization of methylglyoxal synthase from *Clostridium acetobutylicum* ATCC 824 and its use in the formation of 1,2-propanediol. Appl Environ Microbiol **65:**3244–3247.
59. **Liyanage H, Kashket S, Young M, Kashket ER.** 2001. *Clostridium beijerinckii* and *Clostridium difficile* detoxify methylglyoxal by a novel mechanism involving glycerol dehydrogenase. Appl Environ Microbiol **67:**2004–2010. http://dx.doi.org/10.1128/AEM.67.5.2004-2010.2001.
60. **Forage RG, Foster MA.** 1982. Glycerol fermentation in *Klebsiella pneumoniae*: functions of the coenzyme B_{12}-dependent glycerol and diol dehydratases. J Bacteriol **149:**413–419.
61. **Pyne ME, Bruder M, Moo-Young M, Chung DA, Chou CP.** 2014. Technical guide for genetic advancement of underdeveloped and intractable *Clostridium*. Biotechnol Adv **32:**623–641. http://dx.doi.org/10.1016/j.biotechadv.2014.04.003.
62. **Heap JT, Pennington OJ, Cartman ST, Minton NP.** 2009. A modular system for *Clostridium* shuttle plasmids. J Microbiol Methods **78:**79–85. http://dx.doi.org/10.1016/j.mimet.2009.05.004.
63. **Yu MR, Du YM, Jiang WY, Chang WL, Yang ST, Tang IC.** 2012. Effects of different replicons in conjugative plasmids on transformation efficiency, plasmid stability, gene expression and *n*-butanol biosynthesis in *Clostridium tyrobutyricum*. Appl Microbiol Biotechnol **93:**881–889. http://dx.doi.org/10.1007/s00253-011-3736-y.
64. **Wang Y, Zhang Z-T, Seo S-O, Choi K, Lu T, Jin Y-S, Blaschek HP.** 2015. Markerless chromosomal gene deletion in *Clostridium beijerinckii* using CRISPR/Cas9 system. J Biotechnol **200:**1–5. http://dx.doi.org/10.1016/j.jbiotec.2015.02.005.
65. **Xu T, Li Y, Shi Z, Hemme CL, Li Y, Zhu Y, Van Nostrand JD, He Z, Zhou J.** 2015. Efficient genome editing in *Clostridium cellulolyticum* via CRISPR-Cas9 nickase. Appl Environ Microbiol **81:**4423–4431. http://dx.doi.org/10.1128/AEM.00873-15.
66. **Al-Hinai MA, Fast AG, Papoutsakis ET.** 2012. Novel system for efficient isolation of *Clostridium* double-crossover allelic exchange mutants enabling markerless chromosomal gene deletions and DNA integration. Appl Environ Microbiol **78:**8112–8121. http://dx.doi.org/10.1128/AEM.02214-12.